Title

Quantification of colloidal and aqueous element transfer in soils: The dual-phase mass balance model

Authors

Bern, Carleton R
Thompson, Aaron
Chadwick, Oliver A

Publication Date

2015-02-01

DOI

10.1016/j.gca.2014.12.008

Peer reviewed

Available online at www.sciencedirect.com

ScienceDirect

Geochimica et Cosmochimica Acta 151 (2015) 1–18

Geochimica et Cosmochimica Acta

www.elsevier.com/locate/gca

Quantification of colloidal and aqueous element transfer in soils: The dual-phase mass balance model

Carleton R. Bern [a,*], Aaron Thompson [b], Oliver A. Chadwick [c]

[a] Crustal Geophysics and Geochemistry Science Center, U.S. Geological Survey, Denver Federal Center, Denver, CO 80225, USA
[b] Department of Crop and Soil Sciences, University of Georgia, Athens, GA 30602, USA
[c] Department of Geography, University of California, Santa Barbara, CA 93106, USA

Received 21 January 2014; accepted in revised form 5 December 2014; Available online 15 December 2014

Abstract

Mass balance models have become standard tools for characterizing element gains and losses and volumetric change during weathering and soil development. However, they rely on the assumption of complete immobility for an index element such as Ti or Zr. Here we describe a dual-phase mass balance model that eliminates the need for an assumption of immobility and in the process quantifies the contribution of aqueous versus colloidal element transfer. In the model, the high field strength elements Ti and Zr are assumed to be mobile only as suspended solids (colloids) and can therefore be used to distinguish elemental redistribution via colloids from redistribution via dissolved aqueous solutes. Calculations are based upon element concentrations in soil, parent material, and colloids dispersed from soil in the laboratory. We illustrate the utility of this model using a catena in South Africa. Traditional mass balance models systematically distort elemental gains and losses and changes in soil volume in this catena due to significant redistribution of Zr-bearing colloids. Applying the dual-phase model accounts for this colloidal redistribution and we find that the process accounts for a substantial portion of the major element (e.g., Al, Fe and Si) loss from eluvial soil. In addition, we find that in illuvial soils along this catena, gains of colloidal material significantly offset aqueous elemental loss. In other settings, processes such as accumulation of exogenous dust can mimic the geochemical effects of colloid redistribution and we suggest strategies for distinguishing between the two. The movement of clays and colloidal material is a major process in weathering and pedogenesis; the mass balance model presented here is a tool for quantifying effects of that process over time scales of soil development.
Published by Elsevier Ltd.

1. INTRODUCTION

At a fundamental level, the development of soil involves the gain and loss (i.e., mass balance) of chemical elements. Since soils are open systems, neither mass nor volume is constant and thus assessing elemental mass balance over the course of soil development is challenging. One solution to quantifying changes in individual elements has been to reference gains and losses to an index constituent that is assumed stable (immobile) within given bounds. Brimhall et al. developed models describing relationships between mass, volume, and mobile and immobile components (Brimhall et al., 1985, 1988; Brimhall and Dietrich, 1987). That work yielded a concise model that has become a crucial and widely used means for assessing open system mass balance and volumetric change by referencing an index constituent, usually an element presumed to be chemically immobile (Brimhall et al., 1991, 1992; Chadwick et al., 1990). Application of the Brimhall model has allowed Earth scientists to trace mineral weathering and soil development across pedogenic time scales inaccessible through

* Corresponding author. Tel.: +1 303 236 1024; fax: +1 303 236 3200.
E-mail address: cbern@usgs.gov (C.R. Bern).

http://dx.doi.org/10.1016/j.gca.2014.12.008
0016-7037/Published by Elsevier Ltd.

contemporary monitoring, thus contributing to understanding how the Critical Zone evolves and the growing effort to predict its response to natural and anthropogenic perturbations (Brantley and Lebedeva, 2011).

The fundamental idea of using an assumed immobile component to quantify changes in mass, volume, and mobility of elements has a long history, but has undergone relatively little evolution in that time. One early example comes from Merrill (1897) who used Fe or Al as a "constant factor" to determine the percentages of mobile constituents retained and lost in weathered material. A rearranged form of Merrill's equation was used by Reiche (1943) to calculate the fraction of a constituent retained (x):

$$x = \frac{(A_w \cdot C_f)}{(A_f \cdot C_w)} \tag{1}$$

Here A and C are the "weight percentages of the variable and the (assumed) non-variant constituents", respectively and the subscripts refer to weathered (w) and fresh (f) rock (Reiche, 1943). The hazard of assuming constancy was apparent to Reiche, but the technique became a useful tool for indexing weathering losses in rock and soil (e.g., Goldich, 1938; Morgan and Obenshain, 1942; Nesbitt, 1979). Muir and Logan (1982) presented a metric called the eluvial/illuvial coefficient (EIC) to determine chemical change and mass fluxes from soil horizons resulting from pedogenesis. That paper cites Rode (1935) and Barshad (1964) as the source of the method, but in the style of Merrill (1897) includes a separate "parent material quotient" to account for the change in mass relative to the index constituent (Muir and Logan, 1982).

The element immobility problem spurred an interest in using heavy and weathering-resistant mineral phases as an index (Marshall, 1940). Minerals including tourmaline, anatase and rutile were isolated from soil size fractions to serve as indices. Zircon became a favorite because chemical analysis could be substituted for mineralogical analyses by assuming that all Zr occurred in zircon (Marshall, 1940; Marshall and Haseman, 1942). In addition to elemental redistribution, the index mineral concept had potential to account for the translocation of clay, as described by Barshad (1955). One limitation on the adoption of Barshad's models was that they were described only through text, without accompanying equations. Additional limitations were the assumptions of a uniform transformation of nonclay to clay across the soil profile; the absence of clay weathering; and that no clay migrates out of the soil profile (Brewer, 1964).

A complete mass balance model that quantified changes in soil mass, volume, and gains or losses of constituent elements relative to an assumed immobile constituent was presented by Brewer (1964). This model was a synthesis of existing models (Marshall and Haseman, 1942; Nikiforoff and Drosdoff, 1943), and also utilized the "parent material quotient" concept. Brimhall developed a similar model to better understand the enrichment of ores by metasomatism (Brimhall et al., 1985; Brimhall and Dietrich, 1987) and enrichment of bauxite deposits by dust (Brimhall et al., 1988). The applicability of these ideas to other open-chemical systems was apparent, and so they were rapidly adapted to the study of soils and weathering (Brimhall et al., 1991, 1992; Chadwick et al., 1990). A comparison of the Brewer and Brimhall models shows equations that were formulated in different manners, but that obtain the same results. The Brimhall model has now become the standard tool for assessing and interpreting volumetric change and elemental mass balance during soil formation and weathering (Amundson, 2010; Brantley and Lebedeva, 2011).

Derivations of the three major metrics of Brimhall's model can be found in several papers (Brimhall and Dietrich, 1987; Brimhall et al., 1988, 1991; Chadwick et al., 1990). Each of the metrics references an index constituent (i) for which immobility is assumed. Strain ($\varepsilon_{i,s}$) measures changes in volume as the porosity of soil and density of its particulate components change:

$$\varepsilon_{i,s} = \frac{V_s - V_p}{V_p} = \frac{\rho_p C_{i,p}}{\rho_s C_{i,s}} - 1 \tag{2}$$

Here V_p and V_s are volumes of parent material and soil, respectively, and the bulk density (ρ) and concentration of an index component (C_i) are measured for the parent material (p) and soil (s). If, for example, the volume has doubled in the weathered material then $\varepsilon_{i,s}$ is 1.0, and if volume is halved $\varepsilon_{i,s}$ is -0.5.

The open-chemical-system transport function, $\tau_{j,s}$, is the mass fraction of element j added or lost relative to the mass originally present in parent material:

$$\tau_{j,s} = \frac{\rho_s C_{j,s}}{\rho_p C_{j,p}}(\varepsilon_{i,s} + 1) - 1 \tag{3}$$

Thus strain accounts for changes in mass and volume that would otherwise distort element gain or loss. Where 100% of element j has been lost, $\tau_{j,s}$ equals -1.0; where the mass of element j has doubled in the volume considered, $\tau_{j,s}$ equals 1.0.

The mass of element j gained or lost from a given volume of weathered material (m_j), can then be determined by using $\tau_{j,s}$:

$$m_j = \left(\rho_p V_p \frac{C_{j,p}}{100}\right)\tau_{j,s} \tag{4}$$

When using this equation to determine gains or losses from soil profiles, strain must be calculated in order to correctly define the original volume of parent material from which the gain or loss occurred, rather than using the measured volume of the soil horizon (Egli and Fitze, 2000). Brantley and Lebedeva (2011) have formulated another equation incorporating a strain correction based on the measured volume of weathered material rather than the original volume of parent material.

Two minor modifications have been made in the use of $\tau_{j,s}$. First, the equation can be reduced to a simpler form that eliminates the need for bulk density data or a determination of strain:

$$\tau_{j,s} = \left(\frac{C_{j,s}}{C_{j,p}} \times \frac{C_{i,p}}{C_{i,s}}\right) - 1 \tag{5}$$

(Vidic, 1994; Egli and Fitze, 2000; Kurtz et al., 2000). Such a formulation is comparable to Eq. (1) and earlier models for assessing open system mass balance (Reiche, 1943;

Merrill, 1897). It has also been shown (e.g., Vidic, 1994) that $\tau_{j,s}$ yields results identical to the eluvial/illuvial coefficient of Muir and Logan (1982). Second, the effect of the common practice of sieving bulk soil and only analyzing the fines (<2 mm material) has been acknowledged and an attempt made to account for it (Porder et al., 2007a). By assuming that material >2 mm is unweathered and chemically identical to bulk parent material, this method determines the open-chemical-system transport function for element j in the context of bulk soil ($\tau_{j,s}$) by using the concentrations of the index component ($C_{i,w}$) and the element of interest ($C_{j,w}$) measured in the <2 mm fraction, designated by the subscript w. The new formulation also incorporates the term f_w, for mass fraction of fines relative to bulk soil:

$$\tau_{j,s} = \left(\frac{C_{j,w}}{C_{j,p}} \times \frac{C_{i,p}}{C_{i,w}} - 1\right) \times f_w \quad (6)$$

(Porder et al., 2007a). However, as described in the next section, there is an error in this formulation. With the exception of improving how total gains and losses are calculated from soil profiles and the two modifications to calculating $\tau_{j,s}$, the Brimhall model has proven robust and its utility continues to expand as it is incorporated into broader models of soil development (e.g., Riebe et al., 2003; Yoo et al., 2007; Jin et al., 2010).

In practice, models assuming complete immobility for an index element have inherent limitations. The high field strength (HFS) elements Zr, Ti, and Nb are favored as index elements, because their low solubility is equated with low mobility. However, numerous studies have revealed that the HFS elements actually display some degree of mobility (Sudom and St. Arnaud, 1971; Colin et al., 1993; Cornu et al., 1999; Kurtz et al., 2000; Taboada et al., 2006; Jin et al., 2010). Such mobility may stem from redistribution of the clay and colloidal size-fractions through a matrix of larger particles (Sudom and St. Arnaud, 1971; Thompson et al., 2006) or complexation by mobile organic matter (Viers et al., 2000). Conceptually, sand and larger particles can act as a soil skeleton through which a plasma consisting of dissolved material and suspended particles may move (Jenny and Smith, 1935). This idea underpinned the index mineral concept, where weathering-resistant minerals were quantified from distinct size fractions composing the less mobile skeleton (Marshall and Haseman, 1942; Barshad, 1955). Index elements have become the standard approach (Amundson, 2010), but if the index element is mobilized in dissolved or suspended particulate form the resulting mass balance calculation will be compromised. Studies often compare elements prior to selecting the index (Chesworth et al., 1981; Chadwick et al., 1990), but this may simply select the least mobile element.

In this paper, we describe modifications to the mass balance approach that explicitly address suspended particulate (colloid) transfer in soil by utilizing differences in the mobility of HFS elements resulting from differential incorporation into the smallest particle size-fractions. Mass balance requires that preferential redistribution will alter the ratios of the HFS elements in source and accumulation regions, and therefore HFS element ratios of parent material, colloidal material, and soil can be used to trace and quantify the gain or loss of colloidal material for a given soil zone. The model formulations presented here are modified from those described previously (Bern and Chadwick, 2010; Bern et al., 2011) for easier understanding and adoption. Since the model requires estimates of colloid composition, which may not be available from a field context, we present an alternative laboratory-based method for extraction and characterization of colloids from existing soil samples. As an example, we show how the model and the laboratory method can be used to evaluate element redistribution along a catena in South Africa and compare these results with those obtained using calculations assuming Zr immobility. We also illustrate how dust contributions can be distinguished from colloidal redistribution in soils. We intend that the dual-phase model and the associated perspective will provide a new tool for understanding of soils and weathering processes.

2. MASS BALANCE MODEL

2.1. The dual-phase mass balance model

The mass of a given amount of soil (M_s) can be considered as the mass of its (rock) parent material plus the mass gained or lost as dissolved solute material (i.e., aqueous phase, M_d) and gained or lost as solid-phase material suspended in soil water (i.e., colloids, M_c):

$$M_s = M_p + M_d + M_c \quad (7)$$

Such a consideration divides weathering gains and losses, like those estimated from calculations of $\tau_{j,s}$, into two subcomponents, M_c and M_d. This subdivision of soil weathering mass balance is analogous to the manner in which mass balance for soils on eroding slopes has been subdivided. That formulation is:

$$R = D = E + W \quad (8)$$

where R is the rate of rock conversion to regolith, D is the total rate of denudation, E is the flux of bulk soil removed by physical erosion and W is the flux of material removed by chemical erosion (Riebe et al., 2001, 2003). Thus, mass fluxes from the slope are subdivided into physical (E) and chemical (W) components. Such a model assumes the relevant processes are at steady-state and fluxes are rooted in measurements of denudation rates (D) generally determined via cosmogenic nuclides. The weathering flux (W) has largely been considered to represent losses of aqueous solutes because of mobility relative to bulk soil. The dual-phase model presented here is an acknowledgment that colloidal material can also be mobile relative to bulk soil and therefore M_c and M_d together compose the mass change represented by W. The determination of M_c and M_d is therefore independent of physical, erosion-driven gains or losses of bulk soil along a slope, just as the determinations of $\tau_{j,s}$ via the Brimhall model can be made independent of any quantification of erosion. Without a rate measurement, such as denudation rate, the mass changes M_c and M_d are just mass changes, but with a measure of D they could also be converted to rates. As a result, the dual-phase model fits

within—but does not represent—the entire mass balance framework for eroding soils.

The core concept of the dual-phase mass balance model is the use of the elements Ti and Zr as both tracers of the redistribution of the colloidal component, and as an index against which gains and losses of total mass and other individual elements may be assessed. A primary assumption of the model is that Ti and Zr transfer into or out of soil as aqueous solutes is negligible—both elements are essentially insoluble except at pH values much lower than usually attained in soil systems. The dual-phase model determines each of the masses in Eq. (7), as well as the masses of individual elements composing each component (Fig. 1). In some cases, there will be an additional complication of an operationally-defined gravel component (>2 mm material) (M_g), expanding Eq. (7) to:

$$M_s = M_g + M_p + M_d + M_c \tag{9}$$

Such a formulation accounts for the relatively common practice of sieving soils to isolate the fines—generally considered the chemically reactive and therefore weathered component of soil—for chemical analysis. The gravel component is treated as having the composition of unweathered parent material, a frequent although sometimes erroneous assumption in soil studies. That assumption is increasingly being avoided by analyzing unsieved soil, in which case the considerations of M_g presented here can be eliminated.

The mass of soil being considered must be defined first, because all the other masses will be proportional. M_s is defined as:

$$M_s = V_s \rho_s \tag{10}$$

with V_s being soil volume (e.g., a horizon of defined area and thickness) and ρ_s being the density of the bulk soil (both fines and gravel). The fine fraction of soil (M_w), of soil—the portion considered to have been altered by weathering—is defined as:

$$M_w = V_s \rho_s f_w \tag{11}$$

with f_w being the measured mass fraction of material <2 mm in diameter. The subscript w distinguishes material <2 mm in diameter from the soil as a whole, which is designated by the subscript s. As the gravel fraction (M_g) is assumed to be unweathered:

$$M_w = M_p + M_d + M_c \tag{12}$$

and each of the components on the right side of the equation is an unknown variable.

Masses of individual elements in soil and other components are used extensively throughout the dual-phase mass balance model and are denoted with a lower case m (Fig. 1). Using Zr in the soil fines as an example, such masses are determined by:

$$m_{\mathrm{Zr},w} = M_w C_{\mathrm{Zr},w} \tag{13}$$

Here, $m_{\mathrm{Zr},w}$ is the mass of Zr in the mass of soil fines M_w, and $C_{\mathrm{Zr},w}$ is the concentration of Zr in the soil fines. The mass of Zr in parent material that gave rise to the fines ($m_{\mathrm{Zr},p}$) and colloidal material ($m_{\mathrm{Zr},c}$) are similarly defined. Because the transfer of Zr and Ti into or out of soil as aqueous solutes is assumed negligible, no such variable is defined for the dissolved component for those two elements. As a result, the mass of Zr in soil fines ($m_{\mathrm{Zr},w}$) can be defined:

$$m_{\mathrm{Zr},w} = m_{\mathrm{Zr},p} + m_{\mathrm{Zr},c} \tag{14}$$

The mass of Ti in soil fines ($m_{\mathrm{Ti},w}$) can be similarly defined and in both cases the mass of the elements in soil fines is a function of only two variables.

As in previous models, an index is required to reference gains and losses of other elements and Zr is used here for that purpose, but with the gains and losses of Zr via a mobile colloidal component taken into account as described in Eq. (14). Those gains and losses of Zr are determined using formulations borrowed from isotopic

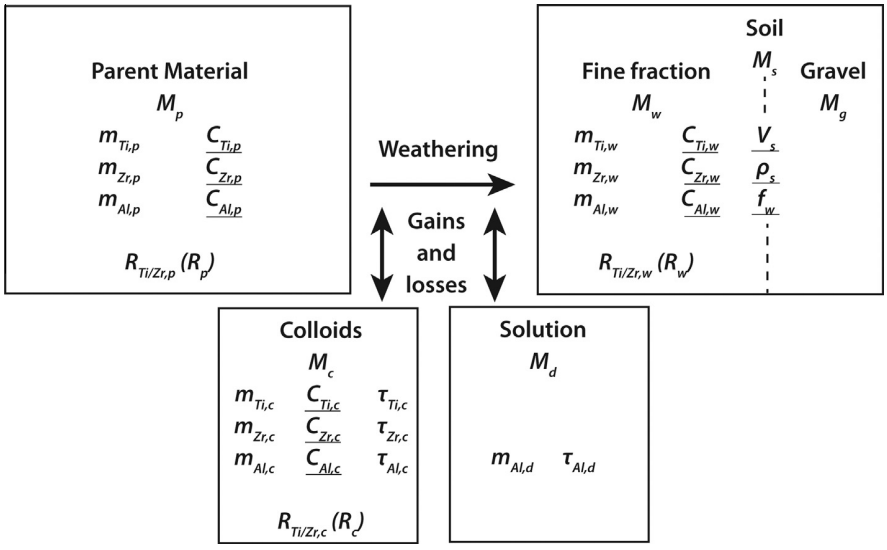

Fig. 1. Illustration of associations between variables in the dual-phase mass balance model. Underlined variables are those that must be measured, all others can be calculated. An individual element for which gains and losses are being determined is represented by Al.

mass balance determinations for two-component mixing (e.g., Capo et al., 1998). However, instead of ratios of isotopes, ratios of Ti to Zr are used to assign proportions to the variables in Eq. (14). Essentially, mass balance requires that if the ratio of Ti to Zr in colloidal material transferred into or out of soil differs from that of the parent material, then the ratio of the two elements in soil will change proportionately. The ratio used to trace such changes is:

$$R_{\mathrm{Ti/Zr}} = \frac{C_{\mathrm{Ti}}}{C_{\mathrm{Zr}}} \tag{15}$$

Here C_{Ti} and C_{Zr} are the concentrations of Ti and Zr, respectively, in a given component. Abbreviating the ratio $R_{\mathrm{Ti/Zr}}$ to R, the ratio of Ti and Zr in the soil fines (R_w) is a function of the ratios (R_p and R_c) in parent material and the colloidal component, respectively, as well as the masses of these elements in each component:

$$R_w = \frac{R_c m_{\mathrm{Zr},c} + R_p m_{\mathrm{Zr},p}}{m_{\mathrm{Zr},c} + m_{\mathrm{Zr},p}} = \frac{m_{\mathrm{Ti},c} + m_{\mathrm{Ti},p}}{m_{\mathrm{Zr},c} + m_{\mathrm{Zr},p}} \tag{16}$$

It is important to note that although both Ti and Zr concentrations are used to calculate $R_{\mathrm{Ti/Zr}}$ values, it is gains and losses of Zr that will be determined in the subsequent formulations. If Ti and Zr are reversed in Eq. (15), gains and losses of Ti will be determined and Ti could be used as the index. Identical model output can be obtained in this manner and thus Ti and Zr fundamentally function as a single index.

The parameter upsilon (υ) is now defined as the proportion of Zr gained or lost from a given mass of soil via the colloidal component:

$$\upsilon = \frac{m_{\mathrm{Zr},c}}{m_{\mathrm{Zr},c} + m_{\mathrm{Zr},p}} \tag{17}$$

where colloidal material has been gained by soil, υ and $m_{\mathrm{Zr},c}$ will be positive, and where colloidal material has been lost, υ and $m_{\mathrm{Zr},c}$ will be negative. By accounting for the mass fraction of Zr attributed to the colloidal component, relative to that mass combined with Zr from parent material, υ provides another means of relating R_w to R_c and R_p.

$$R_w = R_c\upsilon + R_p(1-\upsilon) \tag{18}$$

The ratio of Ti to Zr in soil (R_w) is therefore a linear function of upsilon (υ):

$$R_w = \upsilon(R_c - R_p) + R_p \tag{19}$$

Eq. (19) can be rearranged so that upsilon (υ) becomes a function of R_w, R_p and R_c, all of which can be can be calculated from measured concentrations,

$$\upsilon = \frac{R_w - R_p}{R_c - R_p} \tag{20}$$

The $R_{\mathrm{Ti/Zr}}$ of the various components (soil, parent material, and colloids) can therefore be used to determine the proportion of colloidal Zr mass added or removed from the soil fines. As above, an essentially identical formulation is used to trace the fractional contribution of one component in two-component isotopic mixing (e.g., Capo et al., 1998).The proportionality parameter υ—a function of measured quantities—can then be used to determine the mass of Zr that a soil has gained or lost via colloids by using the mass of Zr in a given mass of soil fines (Eq. (13)),

$$m_{\mathrm{Zr},c} = (m_{\mathrm{Zr},c} + m_{\mathrm{Zr},p}) * \upsilon = m_{\mathrm{Zr},w} * \upsilon \tag{21}$$

With $m_{\mathrm{Zr},c}$ determined relative to $m_{\mathrm{Zr},w}$, $m_{\mathrm{Zr},p}$ can now be determined using the relationship in Eq. (14). Each of those three values can then be used to determine the total mass of material attributable to each component in the relationship by the generic equation,

$$M = \frac{m_{Zr}}{C_{Zr}} \tag{22}$$

In this way, four of the five values in Eq. (9) can be determined: M_s is determined from Eq. (10), M_c is calculated using Eqs. (20)–(22), M_p is calculated from Eq. (22) and the relationship in Eq. (14), and M_g can be determined by substituting the mass fraction of gravel ($f_g = 1 - f_w$) into Eq. (11). Eq. (9) can then be rearranged to solve for the total mass of the dissolved component (M_d),

$$M_d = M_s - M_g - M_p - M_c \tag{23}$$

As the dissolved and colloidal mass changes are considered to only influence the soil fines, one can also determine M_d by

$$M_d = M_w - M_p - M_c \tag{24}$$

As above, values of M_d and M_c will be positive where there have been mass gains, and negative where there have been mass losses. Summing M_d and M_c determines the total mass change that weathering has caused for the mass of soil considered.

Mass gains and losses of individual elements via the colloidal component can be calculated in the fashion of Eq. (13) by simply multiplying M_c by the concentration of the element in colloidal material ($C_{\mathrm{Al},c}$). Using Al as an example,

$$m_{\mathrm{Al},c} = M_c C_{\mathrm{Al},c} \tag{25}$$

A similar calculation can be made to determine the Al present in the parent material that gave rise to the fines ($m_{\mathrm{Al},p}$) and in the soil fines themselves ($m_{\mathrm{Al},w}$). The mass gain or loss of Al in the dissolved phase ($m_{\mathrm{Al},d}$) can then be calculated in the fashion of Eq. (24) by:

$$m_{\mathrm{Al},d} = m_{\mathrm{Al},w} - m_{\mathrm{Al},p} - m_{\mathrm{Al},c} \tag{26}$$

The total mass of Al gained or lost from the mass of soil being considered ($m_{\mathrm{Al},d+c}$) can also be determined:

$$m_{\mathrm{Al},d+c} = m_{\mathrm{Al},p} - m_{\mathrm{Al},w} \tag{27}$$

Such a net mass change term is similar in objective to Eq. (4), but distinctions between the two are described below. To determine the total gain or loss of Al from a soil profile, $m_{\mathrm{Al},d+c}$ may simply be summed for each horizon in the profile.

With mass gains and losses of Al in the dissolved and colloidal components determined, the open-chemical-system transport function for Al can be calculated for those components. For the colloidal component ($\tau_{\mathrm{Al},c}$), the formulation is:

$$\tau_{\mathrm{Al},c} = \frac{m_{\mathrm{Al},c}}{m_{\mathrm{Al},p} + (M_g C_{\mathrm{Al},p})} \quad (28)$$

with $C_{\mathrm{Al},p}$ representing the concentration of Al in parent material (assuming that gravel is chemically identical to parent material). A similar determination can be made for the dissolved component. The mass gains and losses of the colloidal and dissolved components can be combined to determine their net effect by:

$$\tau_{\mathrm{Al},c+d} = \frac{m_{\mathrm{Al},c} + m_{\mathrm{Al},d}}{m_{\mathrm{Al},p} + (M_g C_{\mathrm{Al},p})} \quad (29)$$

This open-chemical-system transport function is similar to that from Eq. (5), but with an important distinction, which is described below.

Accounting for index element mobility using the dual-phase mass balance model has implications for the assessment of volumetric change, as strain (ε) must also be indexed by some component. An adjusted index element concentration in the soil fines restores losses or removes gains due to colloidal redistribution (Bern and White, 2011). Using Zr as the index, the adjusted concentration in soil ($^{*}C_{\mathrm{Zr},w}$) is simply

$$^{*}C_{\mathrm{Zr},w} = \frac{m_{\mathrm{Zr},p}}{m_{\mathrm{Zr},p} + M_w} \quad (30)$$

By incorporating the gravel fraction, an adjusted concentration for the soil as a whole ($^{*}C_{\mathrm{Zr},s}$) can be made by

$$^{*}C_{\mathrm{Zr},s} = \frac{m_{\mathrm{Zri},p} + (M_g C_{\mathrm{Zr},p})}{m_{\mathrm{Zr},p} + M_w + M_g} \quad (31)$$

The adjusted concentration of Zr in soil ($^{*}C_{\mathrm{Zr},s}$) can then be substituted for the index element concentration in Eq. (2). Adjusted soil Zr concentrations can also be substituted into calculations of the chemical weathering flux, "chemical depletion fraction", and weathering rates of individual elements made for soils on eroding slopes (Riebe et al., 2003).

The dual-phase mass balance model has three advantages over previous models. First, it does not assume immobility for any element, a previously necessary assumption increasingly viewed with skepticism (e.g., Colin et al., 1993; Cornu et al., 1999; Kurtz et al., 2000). Titanium and Zr are both assumed to be mobile as suspended solids (e.g., colloids), and mass balance accounts for that mobility. Second, mass gains and losses and the open-chemical-system transport function are divided into dissolved and colloidal components, which links elements to more specific weathering and transport processes. Third, when samples are separated into gravel and soil fines the dual-phase model avoids errors in mass balance accounting.

Whereas the dual-phase mass balance model overcomes the immobility assumption, it is underlain by other assumptions deserving consideration. First among these is the assumption that concentrations of Ti and Zr and their ratio ($R_{\mathrm{Ti/Zr}}$) in colloidal material can be determined in a manner that sufficiently represents colloidal composition over the course of weathering or soil development. An associated requirement is that either Ti or Zr be preferentially partitioned into the colloidal fraction relative to the parent material. The difference between R_c and R_p constitutes the denominator of Eq. (20) and is central to the mass balance calculations. As $R_c - R_p$ approaches zero, uncertainty associated with each value will limit the applicability of the model to a given setting. A second assumption is that negligible amounts of Ti and Zr are redistributed in dissolved forms during weathering. A third assumption is that the parent material is sufficiently homogenous, particularly with regard to Ti and Zr concentrations, that natural parent material heterogeneity does not masquerade as colloidal redistribution. A fourth assumption is that exogenous (e.g., dust) elemental inputs can be taken into account for or are negligible. A fifth assumption is that only the colloidal fraction is mobile relative to bulk soil. If another fraction, (e.g., material <2 μm) is considered mobile relative to bulk soil it may be substituted for colloids in the model. If however there were two differently mobile fractions, perhaps colloids <0.4 μm and clays 0.4–2 μm, then both fractions would need to be expressed separately in Eq. (16) and unique solutions would not be possible in subsequent equations. A sixth assumption is that the gravel fraction is chemically equivalent to the parent material—this assumption can be addressed by not separating the fines from gravel prior to chemical analysis (e.g., Jin et al., 2010) and eliminating the considerations of gravel described above. Finally, because the model relies so heavily on concentrations and ratios of Ti and Zr in a variety of materials, analytical recovery of those elements must be high and it must be assumed that differences between analytical methods do not generate artifacts.

2.2. Comparison to other mass balance models

The nature of mass balance allows the use of a variety of formulations to derive the same information. Eqs. (3) and (5) are one example. Earlier formulations of equations used in the dual-phase mass balance model used the ratio Ti/(Ti + Zr) as a tracer, instead of the Ti/Zr ratio in Eq. (15) (Bern and Chadwick, 2010; Bern et al., 2011; Bern and White, 2011). Such a formulation more clearly acknowledged that Ti and Zr function as a single tracer and index in the model's context, but was identified as potential obstacle to understanding and adoption of the model. Another example comes from Eqs. (6) and (13) in Ferrier et al. (2011), which can be understood to yield the relationship:

$$\frac{M_c}{M_c + M_p} = \left(\frac{C_{\mathrm{Ti},p}}{C_{\mathrm{Ti},w}} - \frac{C_{\mathrm{Zr},p}}{C_{\mathrm{Zr},w}}\right)\left[\frac{C_{\mathrm{Ti},p} - C_{\mathrm{Ti},c}}{C_{\mathrm{Ti},w}} - \frac{C_{\mathrm{Zr},p} - C_{\mathrm{Zr},c}}{C_{\mathrm{Zr},w}}\right]^{-1} \quad (32)$$

In the case of Ferrier et al. (2011), the contribution of dust was quantified, based upon a ratio of Ti to Zr that was distinct from local granitic parent material. The flux terms have been replaced with mass terms and subscripts in the Eq. (32) substitute colloid values for dust values to maintain the conceptual framework established in Section 2.1. Eq. (32) uses principles of mass balance in conjunction with Ti and Zr concentration data to derive some of the same information obtained by the dual-phase mass balance model (Bern and Chadwick, 2010; Bern et al., 2011). Lawrence et al. (2013) and Sommer et al. (2000) also used mass balance models to determine parent material mixing.

An examination of how Eq. (28) accounts for elements in the >2 mm fraction makes it apparent that the modification to the Brimhall model shown in Eq. (6) contains an error. The error occurs because f_w represents the proportion of fines, already depleted in mass at the time of measurement due to weathering, relative to the soil as a whole. A more accurate determination of the open-chemical-system transport function in bulk soil would replace the fraction of fines in soil (f_w) with the fraction of parent material that gave rise to the fines ($M_{<2\mathrm{mm},p}$) relative to total parent material for the volume of soil being considered ($M_{<2\mathrm{mm},p} + M_{>2\mathrm{mm},p}$). Such a fraction can be termed f_p and determined as:

$$f_p = \frac{M_{<2\mathrm{mm},p}}{M_{<2\mathrm{mm},p} + M_{>2\mathrm{mm},p}} = \left(\frac{m_{\mathrm{Zr},w}}{C_{\mathrm{Zr},p}}\right)\left[\frac{m_{\mathrm{Zr},w}}{C_{\mathrm{Zr},p}} + M_g\right]^{-1} \quad (33)$$

Here, Zr is used as the index element. Multiplying by f_p instead of f_w in Eq. (6) will improve the accuracy of the open-chemical-system transport function used in conjunction with analysis of the soil fines by relating the function to unweathered parent material instead of weathered soil. The modification will also improve the accuracy of gains and losses determined by Eq. (4), if $\tau_{j,s}$ is being used instead of $\tau_{j,w}$. However, all of the variables in Eq. (33) are determined without assessment of colloid composition or mobility. Therefore, this method still assumes complete immobility of the index element Zr.

3. METHODS

3.1. Site description

We applied the dual-phase mass balance model to a suite of soil, parent material, and colloid samples from a catena described in Bern and Chadwick (2010) and Bern et al. (2011). Briefly, the catena is in a semiarid, monsoon rainfall regime (~550 mm mean annual rainfall) and extends 150 m along a gentle (⩽5%) slope underlain by Archaean granite and gneiss of the Nelspruit suite within Kruger National Park, South Africa (Barton et al., 1986). Dissolved and suspended material flow through the sandy, quartz-rich skeleton formed from the granitic parent material, and low denudation rates (catchment derived rate = 6.6 ± 1.0 m/m.y., Chadwick et al., 2013) have allowed unusually well-differentiated catenas to form throughout much of the landscape (Venter, 1986; Khomo et al., 2011, 2013). The catena has three zones: a clay-poor upslope position with reddish soils, a clay-poor seepline position with whitish soils, and a clay-rich downslope position with gray-brown soils. The seepline is a narrow strip running parallel to the hillslope contour where subsurface water is forced to the surface during high flow by the clay-rich zone immediately downslope. Seepline soils are highly leached and periodic saturation generates fluctuation redox conditions that have stripped them of iron and clays (Venter, 1986).

3.2. Soil and parent material characterization

Soil and parent material characterization was described in Bern et al. (2011). Briefly, 66 samples from 10 soil profiles were collected from hand-dug pits along the catena. Profiles ST1–3 are located in the upslope zone, profiles ST4–6 are in the seepline zone, and profiles ST7–10 are in the downslope zone. Soil samples were air dried and sieved to <2 mm prior to analysis. Hand samples of local rock types were collected from outcrops close to the catena and beneath saprolite in soil pits. Rock samples included both granitic material thought to best represent soil parent material and mafic xenoliths found primarily in and near outcrops. Weathered rind material was cut from rock samples prior to analysis. Major and trace element concentrations for these soil and rock samples were determined by wave-dispersive and energy-dispersive X-ray fluorescence, respectively, by ALS Chemex (Reno, Nevada). Titanium and Zr concentrations were previously published (Bern et al., 2011) and additional major element data from the same analyses are used here. Data for selected profiles are provided in a Supplementary Table.

3.3. Laboratory characterization of soil colloids

Our previous work relied on characterization of one sample of colloid material collected from water seeping from the upslope soil into a pit dug at the seepline. For this study, we use a simple water extraction of the soils collected from each site and measured the elemental composition of the dispersed colloids and the aqueous phase. New samples of soil were collected from pits dug near profiles ST1 (upslope), ST5 (seepline), and ST9 (downslope) as identified in Bern et al. (2011). The depth increments sampled were 20–40 cm (upslope), 20–40 cm (seepline), and 20–60 cm (downslope), representing eluvial regions in upslope and seepline soils, and an illuvial region in downslope soil. Samples were air dried and sieved to <2 mm.

Triplicate samples from each profile were placed in 250-mL Oak Ridge centrifuge tubes with ultrapure water at a 1:10 soil to solution ratio (23 g of dry soil:207 mL of 18.2 MΩ/cm water). This suspension was shaken for 2 h at 280 rpm on a horizontal shaker (Eberbach 6010). After shaking, we used two separate procedures to isolate the truly dissolved phase and the dispersed colloids.

3.3.1. Isolation of the dissolved phase

The dissolved phase was isolated in two stages to reduce the particle loading on the ultrafilter. In the first stage 12 mL of the shaken suspension was placed in a 12-mL PPCO centrifuge tube and centrifuged at 20,521 rcf for 24 min (Sorvall SM-24 rotor); in the second stage the supernatant of this centrifugation was collected via pipette and added to the top of a pre-cleaned 3KDa ultrafilter apparatus (Millipore Amicon® Ultra). The ultrafilter apparatus was then centrifuged for 40 min (or longer if necessary) at 3567 rcf in a swinging bucket centrifuge (International Equipment Company Model K centrifuge) until 10 mL or more of the solution passed through the filter. The 3KDa filter was then removed and the ~10 mL of ultra-filtered solution was pipetted into a PPCO storage tube and acidified with 6 M HCl (~1% of total volume) to decrease the solution pH below 2 prior to analysis for total elemental concentration on a Perkin Elmer-Sciex 9000 ICP-MS at the University of Georgia.

Because we are interested in measuring metals at trace levels, the 3 kDa ultrafilters and accompanying collection tubes were pre-cleaned to remove excess salts and metals prior to use. The filters were cleaned on the day of use, but the collection tubes were cleaned ahead of time by filling them with 10% ultrapure HCl for 24 h and rinsing the tubes six times with 18.2 MΩ water. On the day of extraction, the 3 kDa filters were inserted into the collection tubes and 10 mL of 10 % ultrapure HCl was added and centrifuged at 3567 rcf for 30 min. in a swinging bucket centrifuge (International Equipment Company Model K centrifuge). The collected solution was discarded and the filter was rinsed six times with 18.2 MΩ/cm water. After reassembly, 10 mL of 18.2 MΩ/cm water was centrifuged through the filters three times with the filter assembly rinsed six times with 18.2 MΩ/cm water in between each centrifugation. The filters can be stored wet for up to 24 h.

3.3.2. Isolation of the dispersed colloids

An ideal target particle size cutoff for mobile colloids is difficult to determine and is likely soil and site specific. For this study, we targeted colloids less than 415 nm because these particles are very likely to pass through the typical 0.45 μm filters commonly used to define soluble (and mobile) portions of the soil porewater. Larger particles are also likely mobile, but we take a conservative approach here to distinguish clearly between colloid mobilization and erosive losses (Chadwick et al., 2013). The centrifugation rate and time for our particle separations are calculated following Stokes Law taking into account the precise minimum and maximum radius of the center top of the suspension and the center bottom of the sedimented soils (Henderson et al., 2012). To isolate the dispersed colloids, the remaining soil suspensions in the 250-mL tubes were centrifuged at 1088 rcf for 3 min (Sorvall F14-6X250y rotor—note this fixed rotor has a low angle (23°) so the calculated force x time necessary to sediment the target particle size is much smaller than for other rotors, which would work equally as well). The supernatant (~190 mL) was carefully extracted via pipette and placed in an acid-washed 250-mL PPCO tube with 1.9 mL of 6 M HCl (ultrapure grade) to reduce the pH of the solution to below 2. This composed the <415 nm particle size separate. Throughout the procedure the mass of all tubes were recorded at each addition or subtraction of soil or solution.

To determine the mass fraction of colloids in suspension ~100 mL of the <415 nm supernatant was added to a pre-weighed Teflon beaker and evaporated to dryness in an HEPA-filtered hood. The resulting dried colloids were then collected and 0.1 g of the sample were added to 0.4 g of $LiBO_4$ and fused at 1050 °C and analyzed by ICP-OES at the Oregon State University. The colloid-specific element concentration was calculated by subtracting the contribution from the aqueous (<3 kDa) fraction. The simple correction used for each element was multiplication of the concentration in dried colloids by the mass fraction of colloids in the <415 nm suspension, subtraction of the aqueous (<3 kDa) concentration, and then division by the mass fraction of colloids in the <415 nm suspension.

4. RESULTS

4.1. Chemical composition of soil colloids

The model assumes redistribution of Ti and Zr in colloidal phases and minimal movement via solution. Thus, their concentrations across the size ranges considered in our dispersion experiments are of particular interest. Aqueous (<3 kDa) elemental concentrations are low (Table 1). The highest replicate average for Ti was 1.1 ± 0.3 ppb at ST5, which compares favorably to the 1.0 ppb concentration measured in the <0.025 μm split of soil water collected *in situ* at position ST5 (seepline) along the catena (Bern et al., 2011). Zirconium was below detection limits for the *in situ* split (Bern et al., 2011), but was present at 0.009 ± 0.005 and 0.017 ± 0.003 ppb, respectively, in the ST1 and ST9 replicates. In contrast, the ST5 replicates had a higher Zr concentration of 1.08 ± 0.04 ppb.

For Ti, Zr, Al, Fe, and many other particle-reactive elements, the contribution from the aqueous fraction to elements in the <415 nm suspensions was <0.1%. However, Na in the aqueous fraction accounted for 38% of Na in the suspensions from downslope soil, illustrating the value of subtracting the <3 kDa contribution from the colloid composition. Resulting sums of element concentrations for individual samples after subtraction of the aqueous contribution calculation were >99.5% of sums prior to the calculation, indicating little overall distortion of colloid composition from the simple correction.

Concentrations of elements in the laboratory-dispersed colloids have low variance between replicates but some notable differences between samples from different catena positions (Table 2). Greater concentrations of Na, Si and Zr, and a low Ti/Zr ratio illustrate a compositional difference between colloids from the seepline position (ST5) and the other two positions. The generally colloid-depleted nature of the seepline soil (Bern et al., 2011) suggests that such a composition may be less representative of colloids across the catena. In contrast, colloids from upslope (ST1) and seepline (ST9) show greater similarities with each other and the sample of colloids sampled *in situ*. As it is not known whether colloids dispersed from soil at a source region (upslope) or accumulation region (downslope) would be more representative of what has been redistributed over long time scales, all six replicates from ST1 and ST9 are averaged for use in the model (Table 2).

4.2. Implementation of the dual-phase mass balance model

4.2.1. Assessing internal consistency of the dataset

The catena has an eluvial portion on the crest and upper side slopes and an illuvial portion farther downslope which allows us to illustrate that the model makes physical sense by demonstrating changes in the ratio $R_{Ti/Zr}$ for a sample of mean granitic parent material composition as it gains or loses proportions of the mean colloidal component (Fig. 2a,b). In this approach, loss of elements via dissolved ions (solutes in the aqueous phase) is simulated by decreasing the total mass of the sample, but holding masses of Ti and Zr constant. Starting from the mean parent material

Table 1
Dissolved (<3 kDa) element concentrations from the colloid dispersion experiments. Values are averages of three replicates per sample. Concentrations below the detection limit are represented by D.L.

Sample	Ca (ppm)	Mg (ppm)	Na (ppm)	K (ppm)	Si (ppm)	Al (ppm)	Fe (ppm)
ST1	0.2	0.1	0.4	0.7	0.2	0.02	0.01
ST5	D.L.	0.8	0.7	1.4	0.2	0.3	0.1
ST9	0.3	0.03	5.1	2.1	0.4	0.01	0.01

Sample	Ti (ppb)	P (ppb)	Sr (ppb)	Ba (ppb)	Mn (ppb)	Zr (ppb)
ST1	0.56	23	0.003	0.005	6	0.009
ST5	1.1	173	0.02	0.008	10	1.08
ST9	0.76	111	0.0004	0.001	0.5	0.017

Table 2
Elemental composition of colloids dispersed in laboratory experiments and other materials considered as part of evaluation of the catena and implementation of the dual-phase mass balance model. Values for the laboratory dispersed colloids (ST1, ST5, ST9) are averages replicates ($n = 3$) for each sample ± the standard error of the mean. The compositions of colloids collected *in situ* from soil water at position ST5 (seepline) along the catena ($n = 1$) and mafic xenoliths ($n = 3$) sampled in nearby outcrops are provided for comparison. The *in situ* colloids were collected from water seeping into a sampling pit and analytical methods are described in Bern et al. (2011). The average composition of colloids dispersed from ST1 and ST9, along with granitic parent material ($n = 12$), are used to calibrate the dual-phase mass balance model and are marked with asterisks.

Sample	Ca (%)	Mg (%)	Na (%)	K (%)	Si (%)	Al (%)	Fe (%)
ST1	0.30 ± 0.01	0.47 ± 0.02	0.34 ± 0.02	1.4 ± 0.1	18 ± 0.5	11 ± 0.5	4.1 ± 0.2
ST5	0.41 ± 0.01	0.296 ± 0.002	1.21 ± 0.04	1.9 ± 0.04	26 ± 0.7	9.8 ± 0.1	2.44 ± 0.03
ST9	0.21 ± 0.01	0.6 ± 0.03	0.19 ± 0.02	1.1 ± 0.1	17 ± 0.8	11 ± 0.6	3.9 ± 0.2
ST1 and ST9 averaged*	0.26 ± 0.02	0.52 ± 0.03	0.26 ± 0.04	1.2 ± 0.1	17.3 ± 0.6	11.2 ± 0.5	4.0 ± 0.2
In situ colloids	0.04	0.1	0.11	1.8	25.8	10.8	2.9
Mafic xenoliths	5.7 ± 0.6	4.6 ± 0.4	2.0 ± 0.2	2.0 ± 0.5	24.7 ± 0.1	6.8 ± 0.2	6.3 ± 0.1
Granitic parent material*	1.6 ± 0.4	0.12 ± 0.04	2.4 ± 0.3	3.2 ± 0.3	33.5 ± 0.5	7.6 ± 0.3	1.5 ± 0.2

Sample	Ti (%)	P (ppm)	Sr (ppm)	Ba (ppm)	Mn (ppm)	Zr (ppm)	Ti/Zr
ST1	0.58 ± 0.03	470 ± 20	100 ± 5	340 ± 20	600 ± 30	61 ± 3	96.0
ST5	0.532 ± 0.005	363 ± 7	158 ± 5	430 ± 10	142 ± 2	156 ± 3	34.0
ST9	0.35 ± 0.02	124 ± 8	61 ± 4	170 ± 10	128 ± 8	36 ± 3	96.9
ST1 and ST9 averaged*	0.46 ± 0.06	300 ± 80	80 ± 10	250 ± 40	360 ± 110	48 ± 6	96.3
In situ colloids	1.1	2414	695	333	161	80	137.6
Mafic xenoliths	0.45 ± 0.03	1200 ± 300	340 ± 70	700 ± 400	1700 ± 130	160 ± 50	28.0
Granitic parent material*	0.12 ± 0.01	240 ± 100	430 ± 70	770 ± 100	230 ± 70	130 ± 7	9.5

composition, losses of dissolved ions will shift samples only in the horizontal direction (x-axis) with the distance proportional to the percentage of mass loss. In contrast, losses of colloidal material will shift the sample generally down the $R_{Ti/Zr}$ axis and gains of colloidal material shift the sample generally up the $R_{Ti/Zr}$ axis. In both cases though the sample moves along paths delineated as solid lines in the figure because Zr is gained or lost as colloidal material, changing the position on the 1/Zr axis.

Using this framework as a reference, the different catena components form a sensible pattern in the model's context (Fig. 2b). Most soil samples with $R_{Ti/Zr}$ values suggesting losses of colloidal material have 20–50% mass losses through dissolution and aqueous transport. In contrast, most samples with $R_{Ti/Zr}$ values suggesting gains of colloidal material have mass losses as aqueous ions in the 10–40% range. Such a pattern is consistent with our current understanding of catena development: zones of colloidal illuviation (gain) are less weathered, while zones of colloidal eluviation (loss) are more weathered. The zones of illuviation would be expected to be less weathered because some water contributed from upslope will have already equilibrated with soil minerals, and accumulation of colloidal clays should restrict water flow and slow dissolution losses (Khomo et al., 2013). Zones of colloidal eluviation would be expected to be more weathered for the opposite reasons.

The alternate explanations for variation in $R_{Ti/Zr}$ along the catena are poorly supported. For instance, variation in $R_{Ti/Zr}$ could arise from mixing of parent materials with different starting values. Mafic xenoliths collected from nearby outcrops have different $R_{Ti/Zr}$ values from granite (Table 2). We simulated the mixing of these two potential parent materials, along with losses of soil mass by dissolution weathering (Fig. 2c). However, many of the catena samples fall outside the domain defined by such a scenario. The samples below the mixing domain could be explained if there were a third parent material component with an $R_{Ti/Zr}$ value much lower than granite that was preferentially incorporated into upslope and seepline soils. However, we

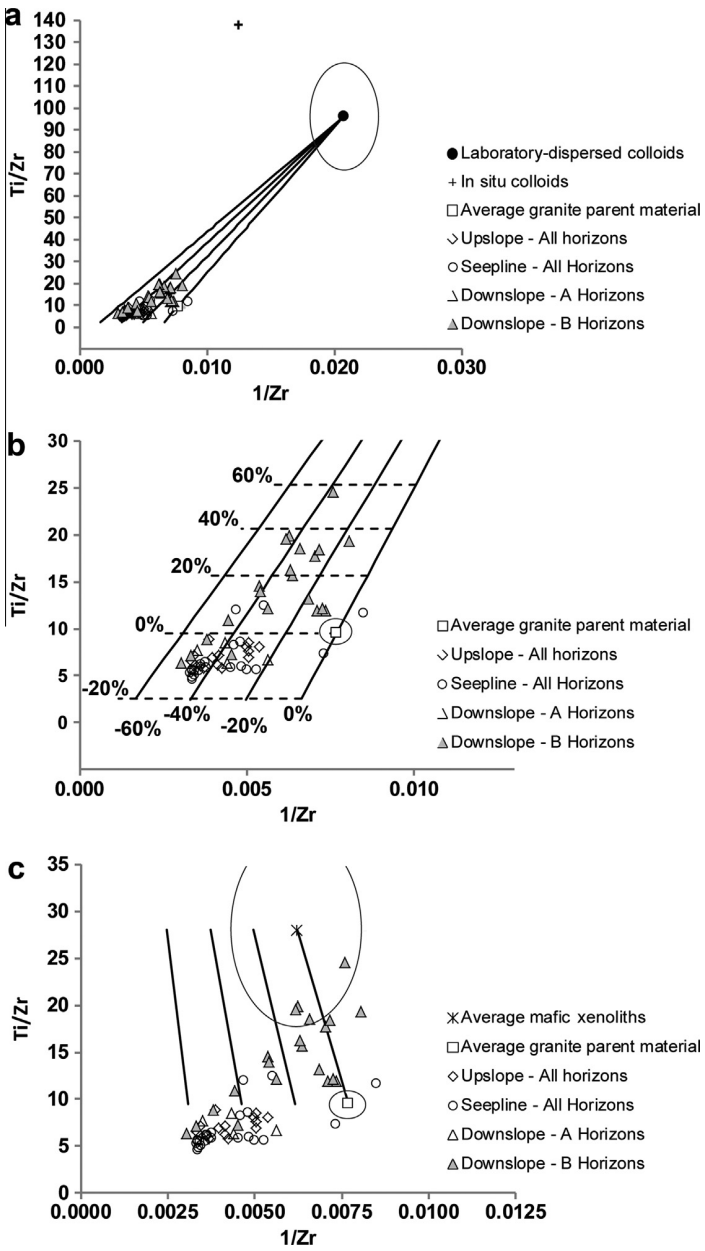

Fig. 2. Measured and simulated sample compositions from the Kruger catena dataset. Measured compositions are plotted as points identified in the legend; solid and dashed lines depict sample compositions simulated for a colloid gain/loss scenario (panels a and b) and a parent material mixing scenario (panel c). Panel (b) is an expanded view of a section of panel (a). Sample compositions simulated for colloid gain/loss are based upon average parent material and colloid compositions given in Table 2, and mass balance relationships defined in the dual-phase mass balance model. Mass losses via solution shift samples only in the horizontal direction and fractional mass losses via solution are shown as percentages. Mass gains and losses via colloids move samples along solid lines through vertical shifts from $R_{Ti/Zr}$ value changes and horizontal shifts from Zr added or removed by colloids. Dashed lines mark percentage of colloid mass gained or lost relative to parent material (M_c/M_p). Solid lines in panel (c) depict mixing between granitic and mafic parent materials. Numbers associated with the solid lines denote the percentage of starting sample mass removed by dissolution. Values falling outside the domain defined by the solid lines indicate that parent material mixing cannot explain all sample compositions. Ellipses in all panels denote the uncertainty associated with rock and colloid compositions. Note that the large size of the ellipse for colloids in comparison to parent material is partly due to greater uncertainty and partly due to greater Ti/Zr and 1/Zr values.

cannot find any low $R_{Ti/Zr}$ contributors to the parent material. Dust from basalt-derived soils influences some granitic Kruger soils where the two are in close proximity (Khomo et al., 2013) but has a high $R_{Ti/Zr}$ value relative to the granitic rocks. Samples falling to the right of the mixing domain would have to be explained as substantial dilution

of Ti and Zr by gains of organic matter or gains of inorganic material via aqueous solutes, but such effects should be subordinate to mass loss in a highly weathered soil. We conclude that colloidal redistribution provides the best explanation of soil Ti and Zr composition.

4.2.2. Comparison to results assuming Zr immobility

The extent of index element mobility along the catena can be assessed using the dual-phase mass balance model. To help make the assessment, the concentration of Zr in bulk soil ($C_{Zr,s}$) can be calculated by:

$$C_{Zr,s} = C_{Zr,w} f_w + C_{Zr,p} f_g \quad (34)$$

again assuming that gravel is geochemically equivalent to parent material and defining $f_g = 1 - f_w$. The difference between that concentration ($C_{Zr,s}$) and the soil Zr concentration adjusted to account for colloidal mobility ($^*C_{Zr,s}$) calculated from Eq. (29) can then be compared to the adjusted concentration (Fig. 3). Upslope and seepline soil horizons have lost up to 5% of their Zr to colloid redistribution, while downslope soils have gained up to 15% relative to parent material. Using Zr as an assumed immobile index would therefore slightly underestimate weathering losses upslope and substantially overestimate them downslope.

Soil strain provides another direct window into the influence of index element mobility on weathering calculations, as the concentrations of other geochemical components are not involved in the calculation of soil strain (Eq. (2)). Strain can be calculated by using Eq. (2) and $C_{Zr,s}$ (assuming Zr immobility) or using $^*C_{Zr,S}$ (accounting for colloidal redistribution). Comparing these two methods illustrates that soil collapse is underestimated slightly in the upslope and seepline positions of the catena, and soil dilation is underestimated substantially where clays have accumulated downslope (Fig. 4).

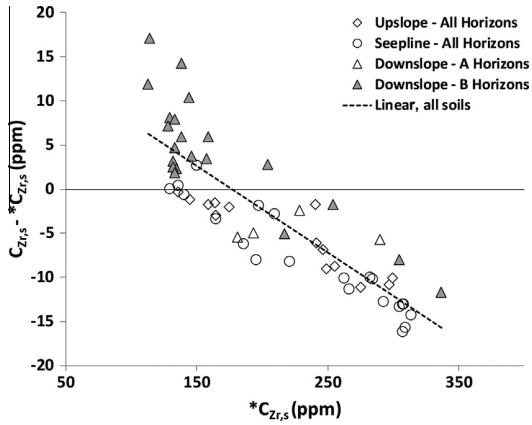

Fig. 3. Difference between unadjusted soil zirconium concentrations ($C_{Zr,s}$) and soil zirconium concentrations adjusted to account for Zr mobility via colloids ($^*C_{Zr,s}$) by using Eq. (29) and plotted versus the adjusted concentrations. Colloid redistribution has altered Zr concentrations along the catena in a manner that will generate systematic errors in metrics such as strain (ε) and the open-chemical-system transport function (τ).

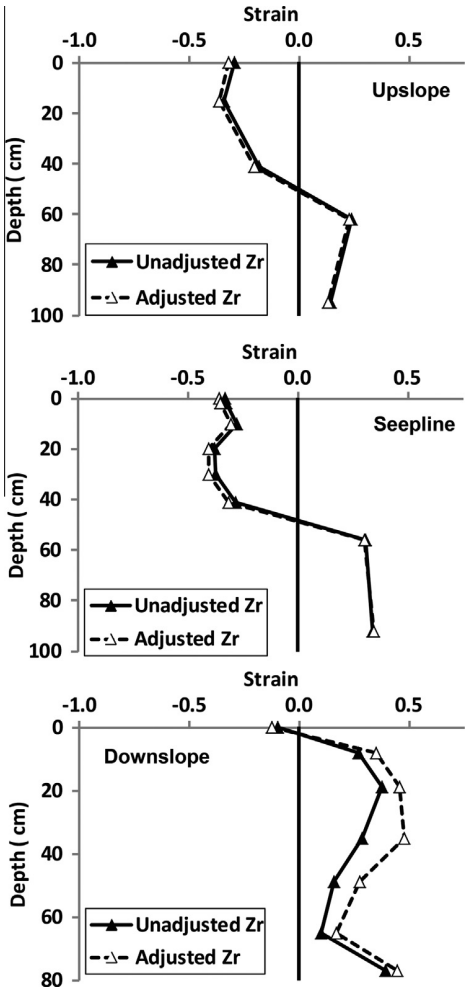

Fig. 4. Strain at positions ST1 (a), ST5 (b), and ST9 (c) along the catena calculated using Eq. (2) and using either $C_{Zr,s}$ (unadjusted Zr) calculated as described in the text, or $^*C_{Zr,s}$ (adjusted Zr) calculated using Eq. (29). Negative strain indicates decreases in volume, with a value of −0.5 indicating a 50% decrease in volume. Positive strain indicates increases in volume, with a volume of 0.5 indicating a 50% increase in volume.

4.2.3. Dissolved and colloidal element redistribution along the Kruger catena

The first level of insight provided by the dual-phase model is simply the overall mass gains and losses that occur via colloids (M_c) vs. dissolved solute material (M_d) relative to the parent material that gave rise to the fines (M_p) (Fig. 2b, Table 3). At the upslope and seepline positions, losses of colloidal material range up to 15% whereas dissolved losses range up to 50%. At the downslope positions, however, gains of colloidal material range up to 56%, and the percentage dissolved losses are generally lower (although values as high as 45% do occur).

Separating the mode of element redistribution provides a much greater level of detail than previous mass balance models (Fig. 5). Solute losses account for the majority of Al, Fe, Si and Na depletion in the upslope and seepline

Table 3
Input variables and dual-phase mass balance model output for three soil profiles along the catena. Output was calculated using parent material and colloid compositions and uncertainties from Table 2.

Catena position	Horizon designation	Depth (cm)	$C_{Ti,w}$ (mg/kg)	$C_{Zr,w}$ (mg/kg)	f_w	ρ_s (kg/m^3)	M_s (kg)	M_w (kg)	M_c (kg)	M_p (kg)	M_d (kg)
Upslope	A	0–15	0.18	291	0.97	1712	257	249	−58 ± 19	578 ± 37	−271 ± 29
	Bw1	15–41	0.19	298	0.95	1812	471	448	−98 ± 35	1061 ± 69	−515 ± 53
	Bw2	41–62	0.17	252	0.90	1764	370	333	−53 ± 22	665 ± 43	−279 ± 33
	2BC	62–95	0.14	198	0.20	1937	639	128	−15 ± 6	200 ± 13	−57 ± 10
	2C	95–105	0.21	292	0.20	1857	186	37	−6 ± 3	86 ± 6	−42 ± 4
Seepline	A	0–2	0.17	277	0.98	1890	38	37	−8 ± 3	82 ± 5	−37 ± 4
	Bw1	2–10	0.17	278	0.96	1890	151	145	−31 ± 11	322 ± 21	−145 ± 16
	Bw2	10–20	0.16	266	0.90	1890	189	170	−40 ± 12	362 ± 23	−153 ± 18
	Bw3	20–30	0.17	299	0.97	1890	189	183	−51 ± 15	440 ± 29	206 ± 22
	Bw4	30–41	0.14	298	0.96	1890	208	200	−69 ± 18	483 ± 31	−214 ± 25
	BC1	41–56	0.15	292	0.77	1890	284	218	−67 ± 18	514 ± 33	−229 ± 26
	BC2	56–92	0.17	267	0.07	1890	680	48	−9 ± 3	101 ± 7	−44 ± 5
	BC3	92–140	0.26	214	0.07	1890	907	64	8 ± 3	101 ± 7	−46 ± 5
Downslope	A	0–8	0.14	227	0.60	2035	163	98	−17 ± 6	177 ± 11	−62 ± 9
	2Btn1	8–19	0.25	142	0.60	1977	217	130	36 ± 6	129 ± 9	−35 ± 7
	2Btn2	19–35	0.26	140	0.50	1854	297	148	44 ± 7	143 ± 10	−39 ± 8
	2Btn3	35–49	0.32	132	0.75	2042	286	214	101 ± 15	180 ± 14	−67 ± 13
	2Bt	49–65	0.32	160	0.75	1952	312	234	93 ± 15	254 ± 18	−112 ± 15
	2BC	65–77	0.28	152	0.50	2220	266	133	44 ± 7	139 ± 9	−50 ± 8
	2Cr	77–88	0.32	162	0.25	1791	197	49	19 ± 3	54 ± 4	24 ± 3

positions. Colloid loss enhances the depletion of Al and Fe more than Si, and has relatively little influence on the depletion of Na. Such patterns are consistent with the solubility of these elements, with the lower solubility elements Al and Fe likely partitioning into nanoparticulate secondary mineral phases and highly soluble base cations (e.g., Na) transported preferentially in dissolved forms. Interestingly, the second, third and fourth horizons down from the surface at the upslope position, and the second through seventh horizons at the seepline position were designated as B horizons of different varieties based upon perceived clay accumulation. Whereas the B-horizon clay may have been

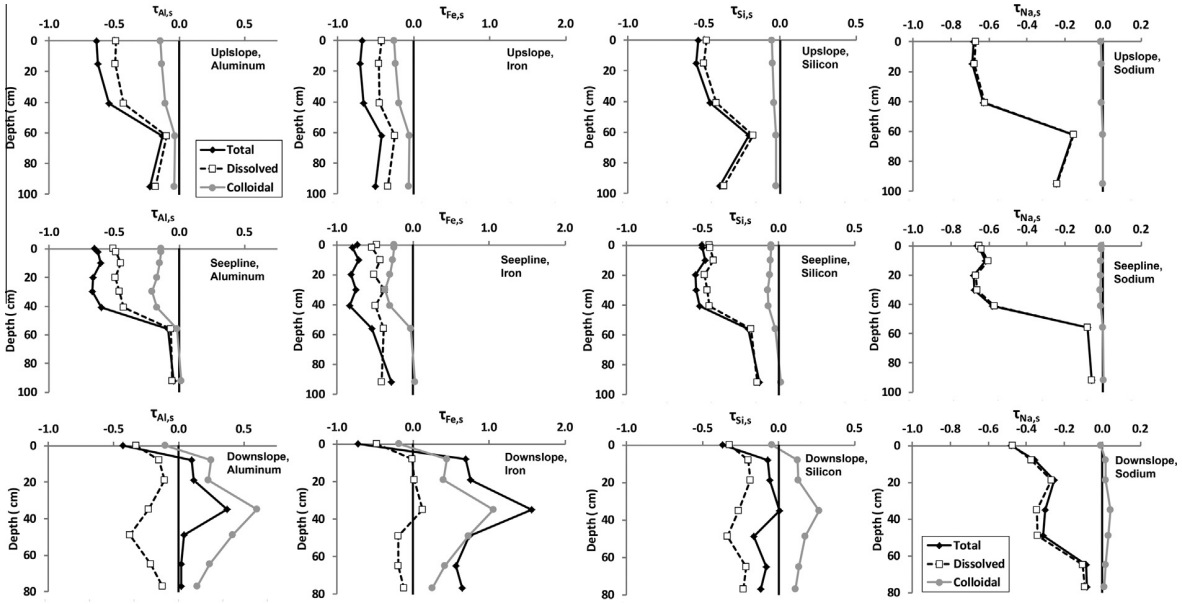

Fig. 5. Depth profiles of model output for Al, Fe, Si and Na (left to right) at profiles ST1, ST5 and ST9 (top to bottom) along the catena. The open-chemical-system transport functions $\tau_{i,c+d,s}$ (total), $\tau_{i,d,s}$ (dissolved) and $\tau_{i,c,s}$ (colloidal) are plotted for each element and distinguished in the legends. The separate contributions of dissolved versus colloidal redistribution to total redistribution can be distinguished for each element.

generated in place or illuviated from overlying or upgradient soil, the dual-phase model suggests these horizons have had a net loss of colloidal material (Table 3, Fig. 5).

The downslope element redistribution patterns are more striking. The dual-phase model indicates solute loss of Al, Si and Na, but gains of these elements via colloid accumulation; whereas it suggests accumulation of Fe via *both* colloid and solute transport. The differences in predicted elemental transfer in the downslope vs. seepline and upslope soils are consistent with the textural differences at these positions. The upslope and seepline soils are sandy and collapsed; whereas the downslope soils are comparatively clay-rich and more dilated. The novelty of our approach is the ability to quantify and compare the magnitude of colloidal versus solute transport for any element along the catena.

4.2.4. Uncertainty in model output

Each of the input variables to the dual-phase mass balance model (Fig. 1) has uncertainty associated with it. Uncertainty associated with variables pertaining to individual soil samples will affect output for only those samples and, unless bias is present in the measurements, will only generate random errors across model output. In contrast, uncertainty associated with the parent material and colloid compositions will generate systematic errors across model output and therefore require more careful consideration. Compared to traditional mass balance determinations that are vulnerable to systematic error only from parent material composition, inclusion of both parent material and colloids in the new model doubles the potential for systematic errors.

Standard errors of the mean associated with Ti and Zr concentrations in parent material and colloids were propagated through the calculations using a Gaussian first-order second-moment approximation approach (e.g., Taylor, 1997). Resulting uncertainty in the calculated mass of parent material of the fines (M_p) is proportionately small, uncertainty in the mass of material lost via solution (M_d) is larger, and uncertainty in the mass of colloids (M_c) is proportionately largest (Table 3). The contribution of uncertainty in colloid composition to output uncertainty is generally smaller than that from parent material. That might seem counterintuitive considering the greater proportionate uncertainty in colloid composition (Table 2, Fig. 2a), but it is a result of $R_{\mathrm{Ti/Zr},w}$ values being closer to $R_{\mathrm{Ti/Zr},p}$ values. As $R_{\mathrm{Ti/Zr},w}$ values deviate further from $R_{\mathrm{Ti/Zr},p}$ values, the contribution of colloid composition uncertainty to output uncertainty increases.

5. DISCUSSION

5.1. The promise of the dual-phase mass balance model

The gains and losses of elements by solute and colloid transport provide valuable clues about the dominant pedogenic processes in hillslope soils (Fig. 5). For instance, although the Kruger catena soils are in a semiarid, monsoon rainfall regime, the soils are likely subjected to strong redox fluctuations, which would solubilize Fe^{2+} and facilitate its downslope transport as an aqueous solute. However the model output suggests that the majority of secondary iron compound accumulation in the lower parts of the hillslope is driven instead by colloidal redistribution, which is consistent with observations that fluctuating redox conditions mobilize colloids (Thompson et al., 2006). In fact, based on the dual-phase model, Al, Si and Na are lost from the downslope soils via solute transport even as they accumulate via colloidal material (Fig. 5). We propose this pattern arises from *in situ* weathering of primary minerals in the downslope profile accompanied by colloid accumulation originating from higher in the landscape where the soils are losing Al, Si and Na as solutes and colloids. Additionally, the lower aqueous solute loss of those three elements in the downslope soils relative to the upslope soils suggests the addition of upslope material is retarding the net weathering loss in the downslope soils.

Current methods to assess clay translocation within a profile or laterally through a hillslope rely on micromorphological studies (Bartelli and Odell, 1960) or short-term experiments and monitoring (El-Farhan et al., 2000). Either strategy can be laborious and fraught with challenges (Nettleton et al., 1969, 1987; Mccarthy and Mckay, 2004) and yet not clearly distinguish the relative magnitudes of solute versus colloid movement. For instance, the prevalence of clay in the downslope position at the Kruger catena is consistent with translocation from the upslope positions, but could also be due to *in situ* formation from transported ions or from recombination of *in situ* weathering products. The dual-phase model readily quantifies a gain of colloidal Al and Si—fingerprinting the translocation process, even while significant solute export occurs. These preliminary interpretations suggest the dual-phase model will have broad utility for quantifying clay translocation and inferring pedogenic processes from soil morphology and present-day chemical composition.

Quantification of Zr redistribution may also help refine determinations of broader measures of soil development that use it as an index. The dimensionless "chemical depletion fraction", $(1-(C_{\mathrm{Zr},p}/C_{\mathrm{Zr},s}))$ divides denudation of soils on slopes between physical erosion of bulk soil and chemical weathering (Riebe et al., 2003), with soil concentrations integrated across vertical profiles. Using measured concentrations of Zr, those values would be 0.41, 0.31 and 0.11 for ST1 (upslope), ST5 (seepline) and ST9 (downslope), respectively, but 0.42, 0.33 and 0.06 if ${}^{*}C_{\mathrm{Zr},s}$ from Eq. (29) is used. Integration of horizons with and without substantial colloid redistribution moderates the differences, but the value is almost halved for ST9. Clearly there will be settings where accounting for colloidal Zr redistribution will improve weathering rate estimates. Where redistribution is systematic with landscape position (Fig. 3), errors can be avoided.

5.2. Considerations for applying the model

Despite the promise of the dual-phase model, certain issues related to the definition of the colloidal component require careful consideration before this model can be widely implemented. First among these is the assumption of a constant mobile colloid pool over the time scales

associated with pedogenesis. The inorganic portions of a mobile colloid pool can be formed through size reduction of primary minerals or through dissolution and subsequent recrystallization (Brady and Weil, 2002). Throughout pedogenesis, the suite of actively weathering minerals changes and likely impacts the composition of potentially mobile colloids. Snapshot characterization of present-day colloids may not be a good representative of the average colloid pool mobilized throughout pedogenesis. Since Ti and Zr occur as trace inclusions or impurities in virtually all minerals (Force, 1976; Nash and Crecraft, 1985), we expect the less recalcitrant minerals will preferentially contribute Ti and Zr to the mobile colloid pool throughout much of soil development. Such release might involve brief, transitional dissolution and precipitation if Ti and Zr are present as impurities in a crystal lattice, or simple physical release of an inclusion as the surrounding matrix weathers. The presence of proportionately more Ti than Zr in easily-weatherable minerals, compared with bulk rock, might account for the observation of proportionately more Ti in the smaller and presumably secondary phases in soil (e.g., Sudom and St. Arnaud, 1971). In contrast, recalcitrant phases in parent material like zircons and rutiles, which undergo more limited chemical and physical weathering in soil, would contribute to the mobile colloidal pool slowly over the full course of pedogenesis (Tejan-Kella et al., 1991). In addition, the influence of plant uptake and cycling of Ti and Zr—albeit small relative to the concentration of these elements in soil (Kabata-Pendias and Pendias, 2001)—may have a distinctive influence over pedogenic timescales.

The second consideration is choosing the position across the landscape and depth within the soil from which to isolate the colloids. For instance, the Kruger catena contains both illuvial and eluvial landscape positions, which exhibit significant variation in colloid composition (Table 2). In this study, we chose an average landscape colloid composition, but depending on what research question is framed, a more specific landscape position may be most appropriate. Likewise, soil texture and structure change with depth and the resulting pore space architecture can also influence the likelihood for colloids to be mobilized, redistributed and/or retained in soil (e.g., Buettner et al., 2014).

The third consideration is the method chosen to physically isolate the colloids from the soil. Various natural biogeochemical and physiochemical processes disperse particles in soils (Grossman and Lynn, 1967; Rousseau et al., 2004), which can mobilize colloids of different compositions (Henderson et al., 2012). The surface charge characteristics of the colloids, especially their point of zero charge (Sposito, 1998) relative to typical soil solution pH, strongly influences their dispersion in response to changes in pH or ionic strength (Kosmulski, 2006). If the expected natural colloid mobilization mechanism is electrostatic, then dispersing colloids from the soil samples by altering the pH or decreasing the ionic strength (by suspending in ultrapure water) may be an appropriate isolation method. However, when colloid dispersion is driven by reductive dissolution of iron oxides this can—though not always (Thompson et al., 2006)—lead to different colloid compositions (Henderson et al., 2012; Buettner et al., 2014), and thus the laboratory isolation mechanism should be adapted to include a Fe-reduction step. Even if the mechanism of natural dispersion can be accurately predicted, the upper particle size limit for mobile colloids can be complicated to define. In one soil column study, Rousseau et al. (2004) found particles <1 μm were generally mobile, but that the average particle size was ~0.45 μm.

For this study, we chose to select the upper colloid size limit by targeting ~0.41 μm based on an average particle density and found some compositional differences from the single *in situ* field sample collected by filtering seepwater through 0.45 μm filters (Bern et al., 2011). Much of the motivation for our uncertainty analysis (Fig. 2) is based on constraining the consequences of using a given colloid composition in the model and these types of analyses are necessary before the dual-phase model can be confidently drawn on to answer a research question.

A final consideration is the magnification in systematic output error (Table 3) as a function of uncertainties in both parent material and colloid compositions (Table 2). One straightforward strategy to assess and reduce those uncertainties is to compile more measurements on both components. The number of measurements required to adequately assess average material composition and associated variability is a topic that is rightfully receiving more attention (Heimsath and Burke, 2013).

Despite these challenges, the dual-phase model provides important information lacking in earlier mass balance model formulations. It will be particularly useful on hillslopes where redistribution of colloidal material should be an important process. Hillslope soils are currently the focus of considerable research thanks to new methods for determining erosion and production rates (Granger and Riebe, 2007), mathematical frameworks for modeling their evolution (Yoo et al., 2007) and increased recognition of their influence on ecosystem biogeochemistry (Porder et al., 2007b). In several existing soil geochemical datasets the fingerprint of colloid redistribution—based on preferential movement of Ti over Zr—suggests colloid mobilization may play an important role in soil development (Green et al., 2006; Jin et al., 2010; Yoo et al., 2011; Yesavage et al., 2012). By correcting for index element mobility (Figs. 3 and 4), dividing elemental mass gains and losses into dissolved and colloidal components (Fig. 5), and better accounting for the standard practice of separating gravel from fines (Eq. (27)), the dual-phase mass balance model could advance our understanding of how hillslope soils form and help us predict their response to environmental change.

5.3. Distinguishing between colloid redistribution and dust accumulation

Changes in the soil Ti/Zr ratio in the Kruger catena are ascribed to the redistribution of colloidal material derived from weathering of the underlying granite, but dust accumulation could also influence this ratio. Implementing the dual-phase mass balance model in strongly dust-influenced settings would result in an erroneous representation

of pedogenesis. Essentially, one must choose between the assumptions that Ti/Zr ratios trace addition of exogenous material or internal redistribution of colloidal material. We illustrate how one might discern between the two scenarios using two previously published datasets (Pilot Peak and Tailholt Mountain) from the Idaho batholith in central Idaho where variations in Ti/Zr ratios were used to quantify the input of mafic-rich Palouse loess-based dust (Sweeney et al., 2007) to granite-derived regolith over time scales of 10^3 to 10^5 years (Ferrier et al., 2011). The analysis of Ferrier et al. (2011) compared rock and regolith individually at 17 sites, whereas all sites on each mountain are lumped in the analysis here.

We simulated a regolith parent material mixing scenario using the Idaho batholith granites and the Palouse loess, and account for loss of regolith mass by dissolution. Plots of 1/Zr versus $R_{Ti/Zr}$ support the conclusion that substantial quantities of Palouse loess ($R_{Ti/Zr} = 62.48$) have been added to the regolith (Fig. 6a,b). On Pilot Peak in particular, the more chemically weathered regolith (lower 1/Zr) has accumulated more dust (higher $R_{Ti/Zr}$) (Fig. 6a), consistent with progressive chemical weathering and dust accumulation over time. However, some regolith samples plot below the average granite material on the $R_{Ti/Zr}$-axis. Loss of colloidal material could explain these samples, assuming a high $R_{Ti/Zr}$ for colloidal material. On Tailholt Mountain, greater dust accumulation coincides with greater chemical weathering, but here numerous regolith samples plot in a zone suggesting dilution of Zr by unknown means (Fig. 6b). Gains of organic matter could dilute Zr concentrations, but parent material variability or geographic variation in granite chemistry across the individual mountains could also influence the pattern.

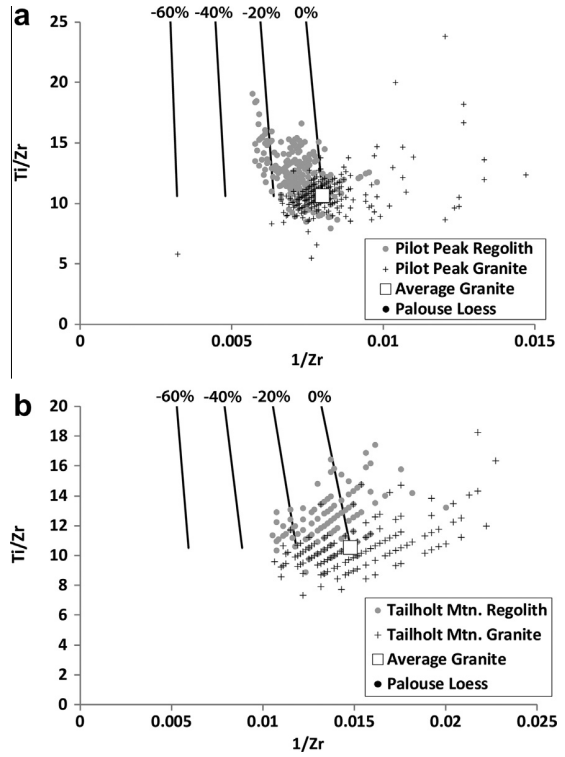

Fig. 6. Measured and simulated sample compositions from the Ferrier et al. (2011) datasets: (a) Pilot Peak; (b) Tailholt Mountain. Measured compositions are plotted as points identified in the legend. Solid lines depict simulated regolith compositions based upon mixing between average granite parent material, and Palouse loess of the composition described by Sweeney et al. (2007) with losses of regolith mass by solution. The Palouse loess mixing component ($R_{Ti/Zr} = 68.48$; $1/Zr = 0.006$) plots outside the defined $R_{Ti/Zr}$ axis ranges. Numbers associated with the solid lines denote the percentage of mass removed by solution. Compare with Fig. 2a,b. Low Ti (<0.05%) and/or Zr (<50 ppm) caused certain granite samples to plot away from the main distribution and therefore 8 of 279 are not included in the analysis of the Pilot Peak dataset, and 53 of 239 granite samples are not included for the Tailholt Mountain dataset. Banding observed in the plots is a discretization effect from rounding of concentration data.

Comparisons between Figs. 2 and 6 show two means by which accumulation of exogenous dust may be distinguished from endogenous redistribution of colloidal material. First, the regolith from the Idaho batholith generally has high $R_{Ti/Zr}$ ratios compared to parent material. The geomorphic setting does not suggest colloid accumulation though, as the regolith was collected from relatively steep (9–40°) slopes on or near ridgelines (Ferrier et al., 2011). Unlike the Kruger catena (Fig. 2), a source zone and accumulation mechanism for colloids therefore appears lacking at the batholith sites. Second, the apparently greater dust accumulation in more highly weathered regolith (Fig. 6) contrasts with the colloid-enriched illuvial zone of the Kruger catena being slightly less weathered than the eluvial source region (Fig. 2). The Idaho batholith pattern makes more sense when viewed as weathering via dissolution and dust accumulation progressing with time. While dust fall undoubtedly occurs at the Kruger catena, and colloid redistribution occurs in Idaho batholith regolith, the perspective presented here can aid in identifying the most influential process operating in a particular setting.

Mineralogical and/or isotopic tracers may also be useful for identifying the influence of dust (Chadwick et al., 2009; Lawrence et al., 2011). Examining element ratios that include other HFS elements such as Hf, Nb, Ta, in addition to Ti and Zr, could also help differentiate exogenous inputs from endogenous redistribution (Kurtz et al., 2000). Using a combination of such strategies, it might even be possible to quantify both processes in the same setting.

6. CONCLUSIONS

Soil and regolith are open chemical and physical systems that expand and collapse in response to additions and removals of mass. Mass balance models that utilize assumptions of index element immobility have increasingly been used to overcome the inherent uncertainties in weathering systems analysis. However, evidence has been mounting that no elements are truly immobile and therefore the assumption of immobility introduces systematic distortions into the mass gain and loss analyses. Here we formulate a model that offers distinct advantages over existing approaches. Rather than assuming immobility, it characterizes the concentrations of high field strength elements in a

colloidal phase that is mobile relative to bulk soil and uses them to evaluate collapse and dilation and to partition the relative gains and losses of other elements by solute (dissolved) and/or colloidal flux. Characterization of the mobile colloidal pool is accomplished here by dispersion in the laboratory—a process that will need to be standardized over time for different soil environments. The reward for the increased analytical effort is increased understanding of pedogenesis. By partitioning element redistribution into solute and colloidal mechanisms we gain much greater detail on the processes and physiochemical conditions responsible for generating present day soil and regolith.

ACKNOWLEDGMENTS

Funding was provided by the Andrew Mellon Foundation. We thank staff at Kruger National Park for access and logistical support. We thank Tony Hartshorn, Liaming Huang, Lesego Khomo, Nehru Mantripragada and Julie Pett-Ridge for assistance both in the laboratory and in the field. Anthony Dosseto, George Hilley, Corey Lawrence, Simon Mudd and Cliff Reibe supplied comments that improved this paper. Any use of trade, product, or firm names is for descriptive purposes only and does not imply endorsement by the U.S. Government.

APPENDIX A. SUPPLEMENTARY DATA

Supplementary data associated with this article can be found, in the online version, at http://dx.doi.org/10.1016/j.gca.2014.12.008.

REFERENCES

Amundson R. (2010) Soil formation. In *Readings from the Treatise on Geochemistry* (eds. H. D. Holland and K. K. Turekian). Elsevier, New York.

Barshad I. (1955) Chemistry of soil development. In *Chemistry of the Soil* (ed. F. E. Bear). Reinhold Publishing Corp., New York.

Barshad I. (1964) Chemistry of soil development. In *Chemistry of the Soil* (ed. F. E. Bear). Reinhold Publishing Corp., New York.

Bartelli L. J. and Odell R. T. (1960) Laboratory studies and genesis of a clay-enriched horizon in the lowest part of the solum of some brunizem and gray-brown podzolic soils in Illinois. *Soil Sci. Soc. Am. Proc.* **24**, 390–395.

Barton, Jr., J. H., Bristow J. W. and Venter F. J. (1986) A summary of the Precambrian granitoid rocks of the Kruger National Park. *Koedoe* **29**, 39–44.

Bern C. R. and Chadwick O. A. (2010) Quantifying colloid mass redistribution in soils and other physical mass transfers. In *Water Rock Interaction* (eds. P. Birkle and I. S. Torres-Alvarado). CRC Press, Taylor & Francis Group, New York.

Bern C. R. and White A. F. (2011) A model for assessing, quantifying, and correcting for index element mobility in weathering studies. *Appl. Geochem.*. http://dx.doi.org/10.1016/j.apgeochem.2011.03.016.

Bern C. R., Chadwick O. A., Hartshorn A. S., Khomo L. M. and Chorover J. (2011) A mass-balance model to separate and quantify colloidal and solute redistributions in soil. *Chem. Geol.*. http://dx.doi.org/10.1016/j.chemgeo.2011.01.014.

Brady N. C. and Weil R. R. (2002) *The Nature and Properties of Soils*. Prentice Hall, Upper Saddle River, New Jersey.

Brantley S. L. and Lebedeva M. (2011) Learning to read the chemistry of regolith to understand the Critical Zone. *Annu. Rev. Earth Planet. Sci.* **39**, 387–416.

Brewer R. (1964) *Fabric and Mineral Analysis of Soils*. John Wiley, New York.

Brimhall G. H. and Dietrich W. E. (1987) Constitutive mass balance relations between chemical composition, volume, density, porosity, and strain in metasomatic hydrochemical systems: results on weathering and pedogenesis. *Geochim. Cosmochim. Acta* **51**, 567–587.

Brimhall G. H., Alpers C. and Cunningham A. B. (1985) Analysis of supergene ore forming processes using mass balance principles. *Econ. Geol.* **80**, 1227–1254.

Brimhall G. H., Lewis C. J., Ague J. J., Dietrich W. E., Hampel J., Teague T. and Rix P. (1988) Metal enrichment in bauxites by deposition of chemically mature aeolian dust. *Nature* **333**, 819–824.

Brimhall G. H., Lewis C. J., Ford C., Bratt J., Taylor G. and Warin O. (1991) Quantitative geochemical approach to pedogenesis: importance of parent material reduction, volumetric expansion, and eolian influx in laterization. *Geoderma* **51**, 51–91.

Brimhall G. H., Chadwick O. A., Lewis C. J., Compston W., Williams I. S., Danti K. J., Dietrich W. E., Power M. E., Hendricks D. and Bratt J. (1992) Deformational mass transport and invasive processes in soil evolution. *Science* **255**, 695–702.

Buettner S. W., Kramer M., Chadwick O. A. and Thompson A. (2014) Mobilization of colloidal carbon during iron reduction events in basaltic soils. *Geoderma*, 139–145.

Capo R. C., Stewart B. W. and Chadwick O. A. (1998) Strontium isotopes as tracers of ecosystem processes: theory and methods. *Geoderma* **82**, 197–225.

Chadwick O. A., Brimhall G. H. and Hendricks D. M. (1990) From a black box to a grey box – a mass balance interpretation of pedogenesis. *Geomorphology* **3**, 369–390.

Chadwick O. A., Derry L. A., Bern C. R. and Vitousek P. M. (2009) Changing sources of strontium to soils and ecosystems across the Hawaiian Islands. *Chem. Geol.* **267**, 64–76.

Chadwick O. A., Roering J. J., Heimsath A. M., Levick S. R., Asner G. P. and Khomo L. (2013) Shaping post-orogenic landscapes by climate and chemical weathering. *Geology* **41**, 1171–1174. http://dx.doi.org/10.1130/G34721.1.

Chesworth W., Dejou J. and Larroque P. (1981) The weathering of basalt and relative mobilities of the major elements at Belbex, France. *Geochim. Cosmochim. Acta* **45**, 1235–1243.

Colin F., Alarçon C. and Vieillard P. (1993) Zircon: an immobile index in soils? *Chem. Geol.* **107**, 273–276.

Cornu S., Lucas Y., Lebon E., Ambrosi J. P., Luizão F., Rouiller J., Bonnay M. and Neal C. (1999) Evidence of titanium mobility in soil profiles, Manaus, central Amazonia. *Geoderma* **91**, 281–295.

Egli M. and Fitze P. (2000) Formulation of pedologic mass balance based on immobile elements: a revision. *Soil Sci.* **165**, 437–443.

El-Farhan Y. H., DeNovio N. M., Herman J. S. and Hornberger G. M. (2000) Mobilization and transport of soil particles during infiltration experiments in an agricultural field, Shenandoah Valley, Virginia. *Environ. Sci. Technol.* **34**, 3555–3559.

Ferrier K. L., Kirchner J. W. and Finkel R. C. (2011) Estimating millenial-scale rates of dust incorporation into eroding hillslope regolith using cosmogenic nuclides and immobile weathering tracers. *J. Geophys. Res.* **116**, F03022. http://dx.doi.org/10.1029/2011JF001991.

Force E. R. (1976) Titanium contents and titanium partitioning in rocks. *U.S. Geol. Surv. Prof. Pap.* **959-A**.

Goldich S. S. (1938) A study in rock-weathering. *J. Geol.* **46**, 17–58.

Granger D. E. and Riebe C. S. (2007) Cosmogenic nuclides in weathering and erosion. In *Treatise on Geochemistry* (eds. H. D. Holland and K. K. Turekian). Elsevier, Oxford.

Green E. G., Dietrich W. E. and Banfield J. F. (2006) Quantification of chemical weathering rates across an actively eroding hillslope. *Earth Planet. Sci. Lett.* **242**, 151–169. http://dx.doi.org/10.1016/j.epsl.2005.11.039.

Grossman R. B. and Lynn W. C. (1967) Gel-like films that may form at the air–water interfaces in soils. *Soil Sci. Soc. Am. J.* **31**, 259–262.

Heimsath A. M. and Burke B. C. (2013) The impact of local geochemical variability on quantifying hillslope soil production and chemical weathering. *Geomorphology* **200**, 75–88. http://dx.doi.org/10.1016/j.geomorph.2013.03.007.

Henderson R., Kabengi N., Mantripragada N., Cabrera M., Hassan S. and Thompson A. (2012) Anoxia-induced release of colloid- and nanoparticle-bound phosphorus in grassland soils. *Environ. Sci. Technol.* **46**, 11727–11734.

Jenny H. and Smith G. D. (1935) Colloid chemical aspects of clay pan formation in soil profiles. *Soil Sci.* **39**, 377–379.

Jin L., Ravella R., Ketchum B., Bierman P. R., Heaney P., White T. and Brantley S. L. (2010) Mineral weathering and elemental transport during hillslope evolution at the Susquehanna/Shale Hills Critical Zone Observatory. *Geochim. Cosmochim. Acta* **74**, 3669–3691. http://dx.doi.org/10.1016/j.gca.2010.03.036.

Kabata-Pendias A. and Pendias H. (2001) *Trace Elements in Soils and Plants*. CRC Press, New York.

Khomo L., Hartshorn A. S., Rogers K. S. and Chadwick O. A. (2011) Impact of rainfall and topography on the distribution of clays and major cations in granitic catenas of southern Africa. *Catena* **87**, 119–128. http://dx.doi.org/10.1016/j.catena.20011.05.017.

Khomo L., Bern C. R., Hartshorn A. S., Rogers K. H. and Chadwick O. A. (2013) Chemical transfers along slowly eroding catenas developed on granitic cratons in southern Africa. *Geoderma* **202–203**, 192–202. http://dx.doi.org/10.1016/j.geoderma.2013.03.023.

Kosmulski M. (2006) PH-dependent surface charging and points of zero charge: III. Update. *J. Colloid Interface Sci.* **298**, 730–741.

Kurtz A. C., Derry L. A., Chadwick O. A. and Alfano M. J. (2000) Refractory element mobility in volcanic soils. *Geology* **28**, 683–686.

Lawrence C. R., Neff J. C. and Farmer G. L. (2011) The accretion of aeolian dust in soils of the San Juan Mountains, Colorado, USA. *J. Geophys. Res.* **116**, F02013. http://dx.doi.org/10.1029/2010JF001899.

Lawrence C. R., Reynolds R. L., Ketterer M. E. and Neff J. C. (2013) Aeolian controls of soil geochemistry and weathering fluxes in high-elevation ecosystems of the Rocky Mountains, Colorado. *Geochim. Cosmochim. Acta* **107**, 27–46. http://dx.doi.org/10.1016/j.gca.2012.12.023.

Marshall C. E. (1940) A petrographic method for the study of soil formation processes. *Soil Sci. Soc. Am. J.* **5**, 100–103.

Marshall C. E. and Haseman J. F. (1942) The quantitative evolution of soil formation and development by heavy mineral studies: a Grundy silt loam profile. *Soil Sci. Soc. Am. J.* **7**, 448–453.

McCarthy J. F. and McKay L. D. (2004) Colloid transport in the subsurface. Past, present, and future challenges. *Vadose Zone J.* **3**, 326–337.

Merrill G. P. (1897) *A Treatise on Rocks, Rock-Weathering and Soils*. The McMillan Company, New York, New York.

Morgan C. G. and Obenshain S. S. (1942) Genesis of three soils developed from materials residual from limestone. *Soil Sci. Soc. Am. J.* **7**, 441–447.

Muir J. W. and Logan J. (1982) Eluvial/illuvial coefficients of major elements and the corresponding loses and gains in three soil profiles. *J. Soil Sci.* **33**, 295–308.

Nash W. P. and Crecraft H. R. (1985) Partition coefficients for trace elements in silicic magmas. *Geochim. Cosmochim. Acta* **49**, 2309–2322.

Nesbitt H. W. (1979) Mobility and fractionation of rare earth elements during weathering of a granodiorite. *Nature* **279**, 206–210.

Nettleton W. D., Flach K. W. and Brasher B. R. (1969) Argillic horizons without clay skins. *Soil Sci. Soc. Am. J.* **33**, 121–125.

Nettleton W. D., Eswaran H., Holzhey C. S. and Nelson R. E. (1987) Micromorphological evidence of clay translocation in poorly dispersible soils. *Geoderma* **40**, 37–48.

Nikiforoff C. C. and Drosdoff M. (1943) Genesis of a claypan soil: I. *Soil Sci.* **55**, 459–482.

Porder S., Hilley G. E. and Chadwick O. A. (2007a) Chemical weathering, mass loss, and dust inputs across a climate by time matrix in the Hawaiian Islands. *Earth Planet. Sci. Lett.* **258**, 414–427.

Porder S., Vitousek P. M., Chadwick O. A., Chamberlain C. P. and Hilley G. E. (2007b) Uplift, erosion, and phosphorus limitation in terrestrial ecosystems. *Ecosystems* **10**, 158–170. http://dx.doi.org/10.1007/s10021-006-9011-x.

Reiche P. (1943) Graphic representation of chemical weathering. *J. Sediment. Petrol.* **13**, 58–68.

Riebe C. S., Kirchner J. W., Granger D. E. and Finkel R. C. (2001) Strong tectonic and weak climatic control of long-term chemical weathering rates. *Geology* **29**, 511–514.

Riebe C. S., Kirchner J. W. and Finkel R. C. (2003) Long-term rates of chemical weathering and physical erosion from cosmogenic nuclides and geochemical mass balance. *Geochim. Cosmochim. Acta* **67**, 4411–4427.

Rode A. A. (1935) To the problems of the degree of podzolization. In *Studies in the Genesis and Geography of Soils* (ed. B. B. Polynov). Dukachaev Institute, Academy of Sciences Press, Moscow.

Rousseau M., Di Pietro L., Angulo-Jaramillo R., Tessier D. and Cabibel B. (2004) Preferential transport of soil colloidal particles: physicochemical effects of particle mobilization. *Vadose Zone J.* **3**, 247–261.

Sommer M., Halm D., Weller U., Zarei M. and Stahr K. (2000) Lateral podzolization in a granite landscape. *Soil Sci. Soc. Am. J.* **64**, 1434–1442.

Sposito G. (1998) On points of zero charge. *Environ. Sci. Technol.* **32**, 11727–11734.

Sudom M. D. and St. Arnaud T. J. (1971) Use of quartz, zirconium and titanium as indices in pedological studies. *Can. J. Soil Sci.* **51**, 385–396.

Sweeney M. R., Gaylord D. R. and Busacca A. J. (2007) Evolution of Eureka Flat: a dust producing engine of the Palouse loess, USA. *Quat. Int.* **162–163**, 76–96. http://dx.doi.org/10.1016/j.quaint.2006.10.034.

Taboada T., Cortizas A. M., García C. and García-Rodeja E. (2006) Particle-size fractionation of titanium and zirconium during weathering and pedogenesis of granitic rocks in NW Spain. *Geoderma* **131**, 218–236.

Taylor J. R. (1997) *An Introduction to Error Analysis*. University Science Books, Sausalito, California.

Tejan-Kella M. S., Fitzpatrick R. W. and Chittleborough D. J. (1991) Scanning electron microscope study of zircons and rutiles from a podzol chronosequence at Cooloola, Queensland, Australia. *Catena* **18**, 11–30.

Thompson A., Chadwick O. A., Boman S. and Chorover J. (2006) Colloid mobilization during soil iron redox oscillations. *Environ. Sci. Technol.* **40**, 5743–5749.

Venter F. J. (1986) Soil patterns associated with the major geological units of the Kruger National Park. *Koedoe* **29**, 125–138.

Vidic N. J. (1994) Pedogenesis and soil-age relationships of soils on glacial outwash terraces in the Ljubljana Basin. Ph. D. thesis, Univ. of Colorado.

Viers J., Dupré B., Braun J.-J., Deberdt S., Angletti B., Ngoupayou J. N. and Michard A. (2000) Major and trace element abundances, and strontium isotopes in the Nyong basin rivers (Cameroon): constraints on chemical weathering processes and elements transport mechanisms in humid tropical environments. *Chem. Geol.* **169**, 211–241.

Yesavage T., Fantle M. S., Vervoort J., Mathur R., Jin L., Liermann L. J. and Brantley S. L. (2012) Fe cycling in the Shale Hills Critical Zone Observatory, Pennsylvania: an analysis of biogeochemical weathering and Fe isotope fractionation. *Geochim. Cosmochim. Acta* **99**, 18–38.

Yoo K., Amundson R., Heimsath A. M., Dietrich W. E. and Brimhall G. H. (2007) Integration of geochemical mass balance with sediment transport to calculate rates of soil chemical weathering and transport on hillslopes. *J. Geophys. Res.* **112**, F02013. http://dx.doi.org/10.1029/2005JF000402.

Yoo K., Weinman B., Mudd S. M., Hurst M., Attal M. and Maher K. (2011) Evolution of hillslope soils: the geomorphic theater and the geochemical play. *Appl. Geochem.* **26**, S-149–S-153. http://dx.doi.org/10.1016/j.apgeochem.2011.03.054.

Associate editor: Anthony Dosseto